3. TAILORING THE CHEMICAL PROPERTIES OF 4 ARM STAR SHAPED POLY(D,L-LACTIDE)

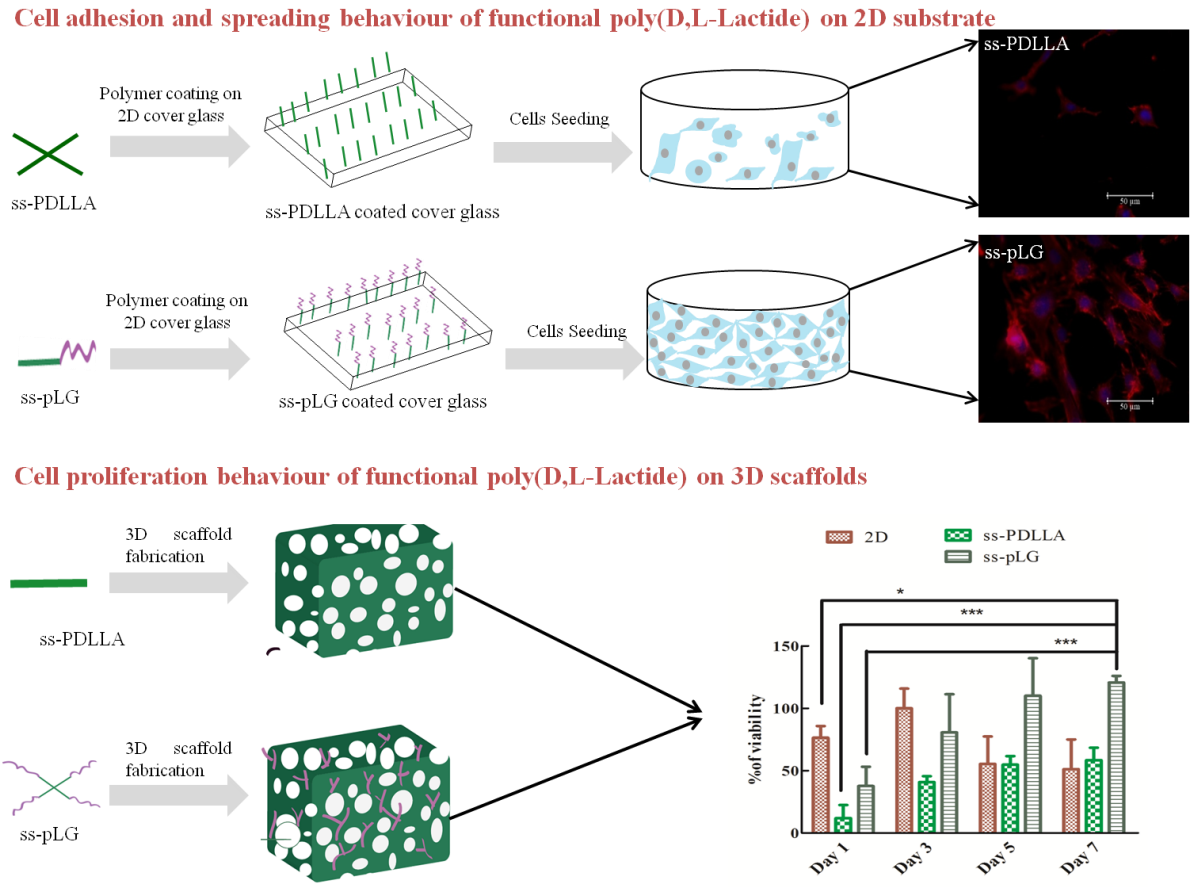

This chapter describes about tailoring the chemical properties of 4 arm star shaped poly(D,L-Lactide) (ss-PDLLA) to make it cell adhesive and its characterization.

3.1. OUTLOOK

Over the past few years, researchers have been strongly focusing on studies related to cell-material interactions to understand the cellular functions and behaviour in response to the materials[76]. Such materials initially serve as a physical support for the cells to facilitate adhesion followed by manifestation of subsequent cellular functions, including proliferation, migration and differentiation [77, 78]. Plethora of literatures is available on biodegradable polymers with an increasing research effort particularly in the last ten years. Yet there has been no corresponding rise in their final commercial end products useful for tissue regeneration4 indicating, cell-material interface science needs more attention towards developing such novel biomaterials in a better and efficient way. Therefore, cell − material interface science needs more attention towards developing novel biomaterials that meets the industrial demands. Therefore, designing a scaffold to control the cell-material interactions could be highly important for the successful development of 3D matrix for tissue engineering applications.

4 arm star shaped PLA representing one of the branched structures of PLA,[79] exhibits various important properties of tissue engineering scaffolds such as chemical multifunctionality [80], low viscosity[81] and higher degradation rate[82, 83] compared to their linear counterpart. However, the hydrophobic nature of PLA surface does not promote cell adhesion thereby hampering its applications in tissue engineering[84]. Initial response of the cells to the scaffold is dependent on the surface properties since material's surface is the first site of cellular contact. Thus, the ability of supporting cell adhesion is the prerequisite for any material to serve as the tissue engineering scaffold. In a natural environment, cell-membrane interaction occurs through integrin binding

sequences of ECM proteins, including RGD, YIGSR, REDV, etc[85]. Therefore, immobilizing adhesive ECM proteins such as fibronectin, laminin and their functional putative peptides (Arg-Gly-Asp (RGD) and Tyr-Ile-GlySer-Arg (YIGSR)) as well as other biocompatible molecules including gelatin and chitosan to the surface of materials is considered to be an innovative approach to control cell adhesion[86, 87].

Many surface-modification techniques have been reported to enhance the biocompatibility and cellular properties of PLA, that include polymerization grafting[88, 89], ozone oxidization[90], plasma modification[91, 92], physical entrapment of cell adhering molecules[93], hydrolysis,[94], aminolysis,[88, 94], surface coating[95] and layer-by-layer self-assembly[96, 97]. Notably, gelatin modification onto PLA substrates has been reported by photografting, surface initiated Atom Transfer Radical Polymerization (ATRP) based chemical grafting and plasma treatment[98-100]. All such modifications are usually done after the fabrication of either films or scaffolds. To the best of our knowledge very few articles report the scaffold fabrication using copolymers of RGD / RGD mimicking peptides coupled biodegradable polymers such as PLA and PCLA (poly(3-caprolactone-co-lactide))[63, 101]. Here, we have assessed a hypothesis that 3D scaffolds fabricated from gelatin grafted 4 arm star shaped poly(D,L-Lactide) (ss-pLG) copolymer may support the cell growth and proliferation more appropriately, as explained in **Figure 3.1**. In particular, cells can migrate deep into the fabricated 3D scaffolds and form the 3D interconnected cell community; whereas such interconnected cell community is highly unlikely to be achieved through other surface modification techniques. As of now, no such study has been reported for controlling the cell adhesion by ss-pLG.

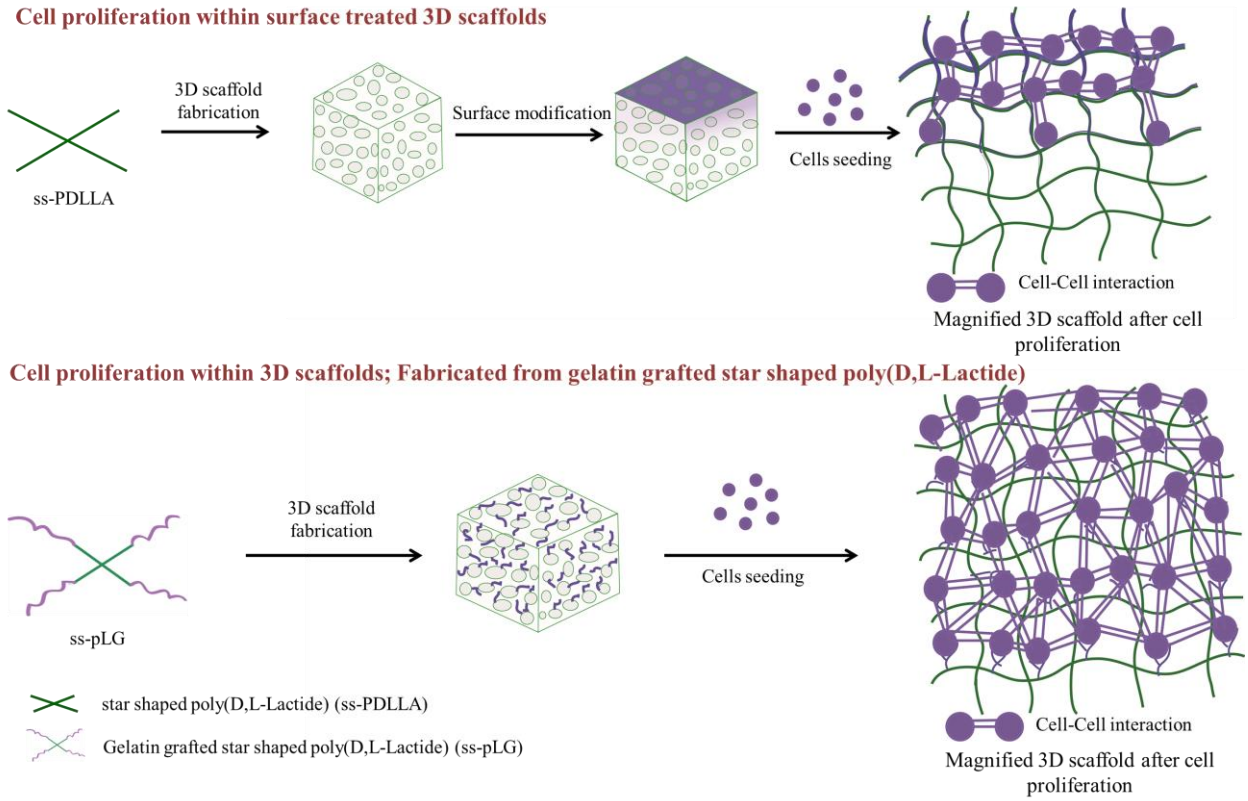

Figure 3.1 Schematic representation of cell proliferation within the surface treated scaffolds and the scaffolds fabricated from gelatin grafted polymers. In case of surface-treated 3D scaffolds, it is likely that distribution of modified entities will be largely non-uniform throughout the scaffold. In such scenarios, introduction of treating moieties is generally found hindered towards the core region of the scaffold. Whereas in case of 3D scaffolds fabricated from gelatin coupled polymers, gelatin is expected to be present in situ within the entire region of the scaffold uniformly since it is already grafted with the backbone of PDLLA. Thus, the fabricated scaffolds are thought to facilitate interconnected 3D cellular networks throughout the matrix.

In the present study, tailoring the chemical properties of star shaped PDLLA (ss-PDLLA) by gelatin grafting and their ability of supporting cellular growth on the modified polymers is demonstrated. It is known that one can control the wettability of PLA by branching [102] and coupling it with some hydrophilic polymers such as poly(ethylene glycol)[103], poly(N-vinylpyrrolidone)[21, 62], gelatin[87, 98], etc

through chemical reactions. As a result, PLA can be tuned preferentially from super-hydrophobic to moderately hydrophilic. We used gelatin (a denatured protein of collagen that has the integrin binding receptor such as DGEA[104]), for modulating the wettability and cell adhesion behaviour of ss-PDLLA polymers. Therefore, herein we report the synthesis and characterization of ss-PDLLA and ss-pLG, followed by fabricating them into 3D scaffolds by freeze drying technique. Considering the advantage of hydrophilicity after gelatin grafting to different arms of PDLLA, we propose that ss-pLG could be a versatile platform for the proliferation of cells in 3D environment with tuneable cellular behaviour and responses. In order to evaluate our hypothesis and to use our ss-pLG scaffolds for tissue engineering applications, we cultured 3T3-L1 cells on ss-pLG polymeric scaffold; unmodified ss-PDLLA scaffold was used for the comparative study.

3.2. RESULTS AND DISCUSSION

3.2.1. Synthesis and characterization of gelatin grafted copolymer (ss-PDLLA-b-Gelatin)

Methods for the synthesis of ss-PDLLA followed by ss-pLG are shown in **Figure 3.2**, where we used combined ring opening polymerization (ROP) followed by end functionalization of gelatin by carbodimide chemistry. Initially, 4 arm ss-PDLLA was synthesized *via* our earlier reported method,[62] where ROP of D,L-Lactide was done in bulk at 150 °C using pentaerythritol as initiator and $Sn(Oct)_2$ as catalyst with the molar feed ratio of D,L-Lactide to pentaerythritol at 693.3. ss-PDLLA polymer synthesis was confirmed by the shifting of the methine proton of D,L, Lactide from 5.3 to ss-PDLLA 5.1-5.2 ppm and the appearance of an additional peak at 4.2 which

corresponds to the methylene protons of pentaerythritol. M_n (NMR) and conversion (NMR) was found to be 1,86,300 g mol^{-1} and 97.2% respectively (**Figure 3.3A(a)**). M_n (GPC) and M_n/M_w of the synthesized polymer calibrated against PMMA standard was 3,79,000 g mol^{-1} and 1.9 respectively (**Table 3.1**).

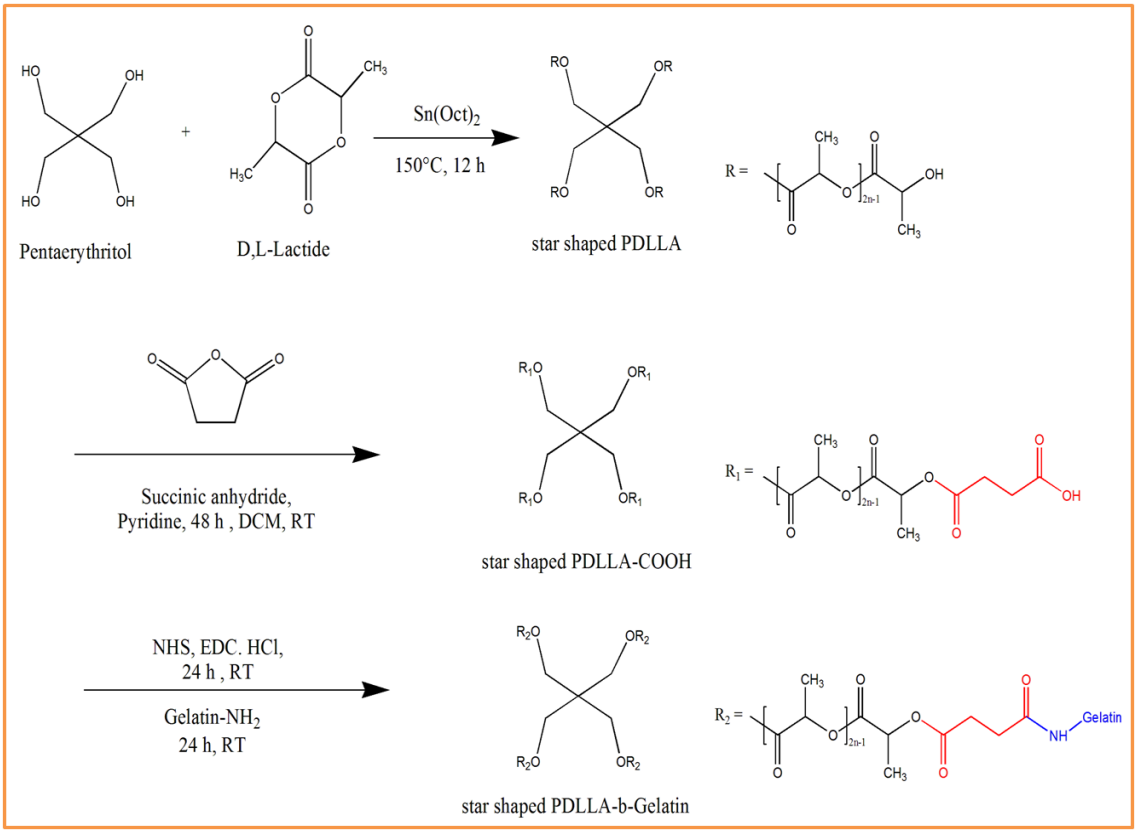

Figure 3.2 Reaction scheme for the synthesis of ss-pLG by ROP using pentaerythritol as initiator and carbodimide mediated end functionalization methods.

To graft the gelatin into ss-PDLLA arm, carboxyl terminated PDLLA was first synthesized by ring opening of succinic anhydride using ss-PDLLA-OH. The appearance of new peaks at 3.6 (*g*+*h*) comes from the methylene protons of succinic anhydride and the disappearance of end terminal methine proton of ss-PDLLA at 4.36 confirms successful ring opening reaction (**Figure 3.3A(b)**).Gravimetric yield of the

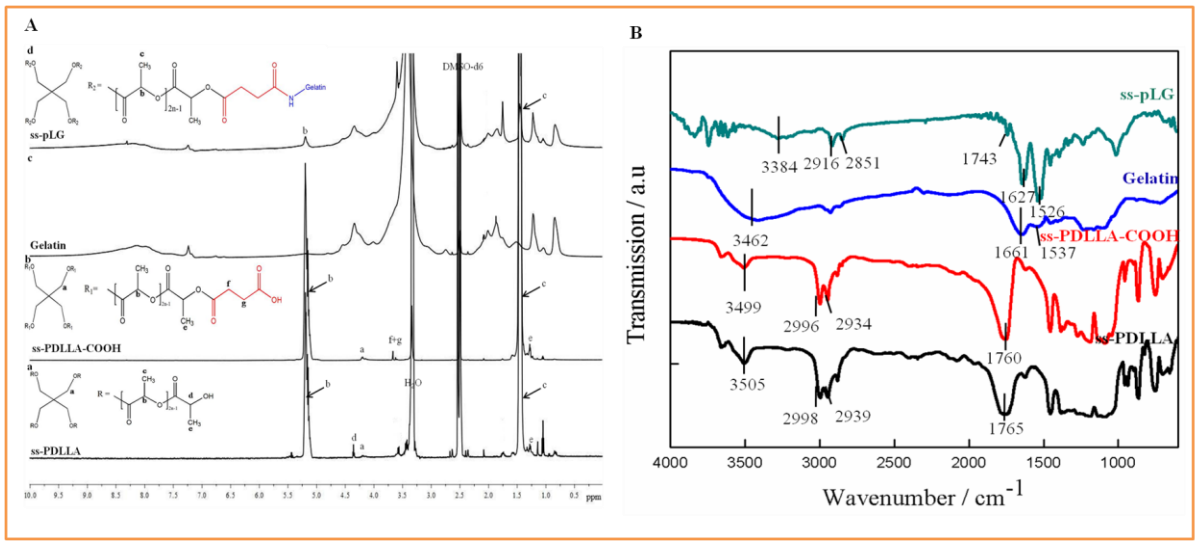

Figure 3.3 Characterization of ss-pLG by ^{1}H NMR and FTIR: (A) ^{1}H NMR spectra of star shaped polymers namely ss-PDLLA, ss-PDLLA-COOH, Gelatin and ss-pLG. (B) FTIR spectra of the respective series of star shaped polymers.

Table 3.1 GPC Characteristic data star shaped PDLLA

Sample	**Conversion (%)[a]**	***M*n(NMR)[b]**	***M*n(GPC)[c]**	***M*n/*M*w**
ss-PDLLA	97.2	186300	379000	1.9

[a] Conversion was determined by comparing the peak area of the residual poly(D,L-Lactide) ~ 5.1-5.2 and monomer D,L-Lactide ~ 5.3 ppm using ^{1}H NMR

[b] Determined from ^{1}H NMR by comparing the methylene proton of pentaerythritol and methine proton of ss-PDLLA at ~ 4.2 and ~ 5.1-5.2 ppm for ss-PDLLA

[c] Determined by GPC (DMF, 0.5 mL/min, 40 ºC) calibrated against PMMA standards

carboxylated ss-PDLLA was found as 74.5 %. The end terminal –COOH group was activated by EDC.HCl and NHS followed by coupling with gelatin was done at unit

molar feed ratio of 1 (PDLLA-COOH to Gelatin). The chemical coupling was confirmed by ^{1}H NMR (Figure S1), where apart from the characteristic peaks of gelatin, characteristic peaks of ss-PDLLA at 5.1-5.2 and 1.46 ppm corresponding to the backbone methine and pendent methyl protons, respectively, are present (**Figure 3.3A(d)**).

Gelatin grafting to ss-PDLLA backbone was further analysed by FTIR spectroscopic technique. **Figure 3.3B** shows the respective FTIR spectra of ss-PDLLA-COOH, gelatin and ss-pLG. ss-PDLLA showed its characteristic peaks at 2998, 2939 and 1765 cm^{-1} which corresponds to asymmetric, symmetric stretching of CH_2 and carbonyl stretching, respectively[105]. (**Figure 3.3B**). When ss-PDLLA-OH opened succinic anhydride ring, characteristic shifting was found from 1765 to 1760 cm^{-1}. Pure gelatin showed the characteristic peaks at 1537 (amide II), 1661(amide I) and 3462 cm^{-1} for its distinct C=O bond vibrations and coupling of bending of N–H bond and stretching of C–N bonds, respectively [106]. After coupling of gelatin into ss-PDLLA back bone, these amide stretching peaks shifted to lower frequencies at 3284 and 1627 cm^{-1}. This observation suggests that $–NH_2$ group of gelatin has successfully coupled with the -COOH group of ss-PDLLA. ss-pLG also showed the characteristic peaks of ss-PDLLA at 2916, 2851 and 1743 cm^{-1} which further supports that ss-PDLLA backbone is present in ss-pLG polymer, whereas the intensity of peak at 1743 cm^{-1} corresponding to the carbonyl stretch of ss-PDLLA backbone was weak. It might be due to the higher content of gelatin or wrapping of ss-PDLLA by gelatin in the ss-pLG.

3.2.1.1. Crystalization behaviour of ss-pLG

X-ray diffraction pattern of Gelatin, ss-PDLLA and ss-pLG is shown in **Figure 3.4**A. Gelatin and unmodified polymers ss-PDLLA showed no sharp peak in XRD pattern, which indicates their amorphous nature. There was no change in crystallinity was observed even after grafting of gelatin into the ss-PDLLA backbone. However, there is significant peak shift was observed which could be definitely due to the gelatin grafting into the 4 arm of PDLLA back bone. XPS confirmed the presence of gelatin in the ss-pLG polymer as the large increase in intensity of nitrogen and the shift in the binding energy, whereas ss-PDLLA did not show any peak respective for the nitrogen in XPS spectrum (Data not shown) (**Figure 3.4**B) [63].

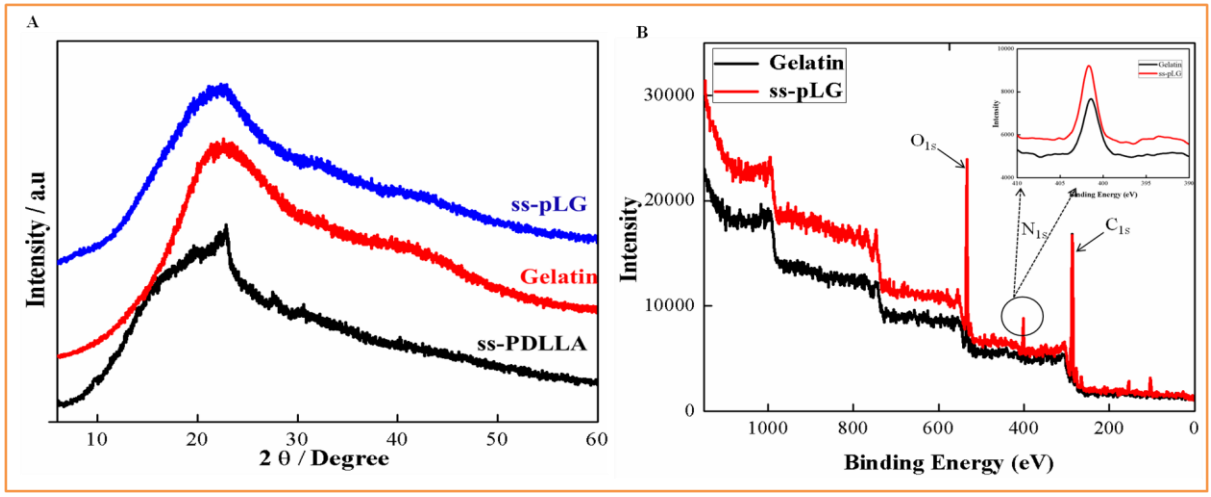

Figure 3.4. Crystallinity of ss-pLG. (A) XRD and (B) XPS spectrum of synthesized polymers compared to unmodified polymer.

3.2.1.2. Thermal peroperties of ss-pLG

The thermogravimetric analysis (TGA) of ss-PDLLA, Gelatin, ss-pLG are presented in **Figure 3.5**A. Thermal degradation profile of gelatin modified and unmodified polymers were quite different. It can be seen that unmodified polymers ss-PDLLA and gelatin

showed T_{onset} at 241 and 285 °C whereas T_{max} of the polymers were found to be 300 and 457 °C respectively. On the other hand, the modified copolymer ss-pLG showed improved thermal properties than their original unmodified polymers. T_{max} of ss-pLG was found to be 455 °C which was almost equivalent to the gelatin (**Figure 3.5**A). This thermal behaviour may be attributed due to the strong coupling of gelatin onto the ss-PDLLA back bone. Moreover, ss-pLG show two different distinct degradation peaks owing to the PDLLA and gelatin block. From this observation, it is clear that the modified ss-pLG has better thermal stability than their unmodified ss-PDLLA.

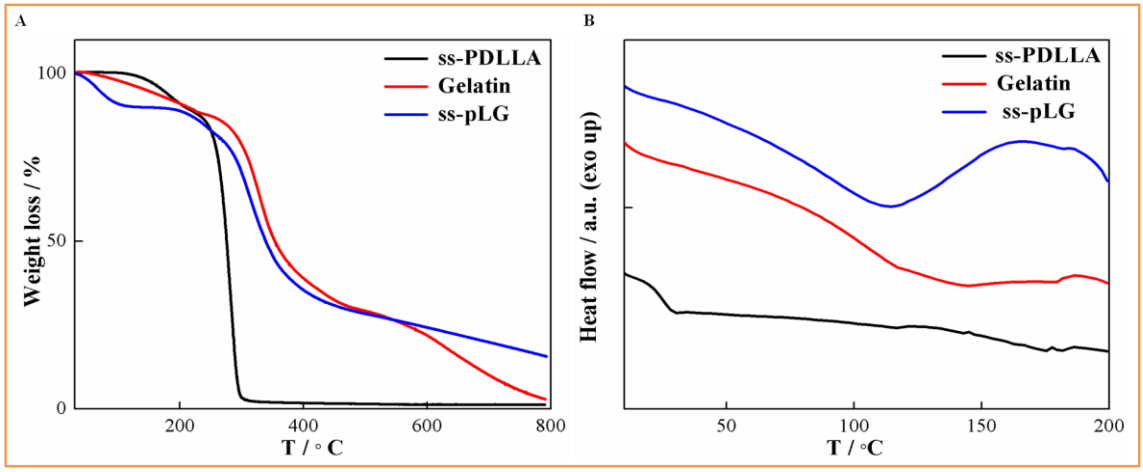

Figure 3.5. Thermal properties of ss-pLG (A) TGA and (B) DSC of series of star shaped polymers namely gelatin, ss-PDLLA and ss-pLG.

DSC thermograms of ss-PDLLA, gelatin and modified ss-pLG are shown in **Figure 3.5**B. In second heating run, T_gs of ss-PDLLA, gelatin, and ss-pLG were observed at 30.36, 142.9, and 112.59 °C, respectively. None of the star shaped evaluated polymers showed melting endotherms or crystallization exotherms which suggests that the ss-PDLLA or gelatin coupled ss-PDLLA (ss-pLG) are highly amorphous in nature. Moreover, because of the grafting of gelatin into PDLLA, clear shifting of T_g was

observed from 30.36 to 112.59 °C for ss-pLG. The observed higher shifting in ss-pLG clearly indicates the presence of higher amount of gelatin in the PDLLA arm (ss-pLG).

3.2.2. Influence of gelatin grafting on protein adsorption and cell adhesion

Gelatin is a natural protein that possesses inherent integrin binding sites and known for the cell adhesion properties. Therefore, we demonstrate this property of gelatin by chemically grafting it to star PDLLA (ss-PDLLA) backbone. Before cell culturing, effects of gelatin on different polymer arms were examined for the protein adsorption efficiency. 12 % polymer films were made from ss-PDLLA and ss-pLG polymers, and further evaluated for their protein adsorption property. Both the films were incubated in BSA after they were wet in PBS completely. ss-pLG film showed higher adsorption, which was 2.6 folds greater owing to its hydrophilicity compared to ss-PDLLA (**Figure 3.6**A). On the other hand contact angle of ss-pLG was 2 folds higher than gelatin (35.81 º). It is important to note that ss-PDLLA also exhibits noticeable adsorption of BSA, most likely due to its hydrophilic property compared to linear PDLLA (data not shown) [102, 107] (**Figure 3.6**B). These results indicate that gelatin modified PDLLA (ss-pLG) facilitate higher degree of protein adsorption which is a crucial parameter required during cell culturing process.

In order to assess the effects of cell−material interactions as well as cell-cell interactions, 3T3-L1 cells were cultured on three different substrates (gelatin, ss-PDLLA and ss-pLG) at low seeding densities. Typically, the focal adhesions contain transmembrane proteins *i.e.* integrin $\alpha_v\beta_3$ as well as plaque proteins (paxillin, vinculin etc.), which connect the cells to underlying substrates. Hence, determination of focal contacts can be used as an index of cell adhesion strength. Vinculin is a cytoskeletal

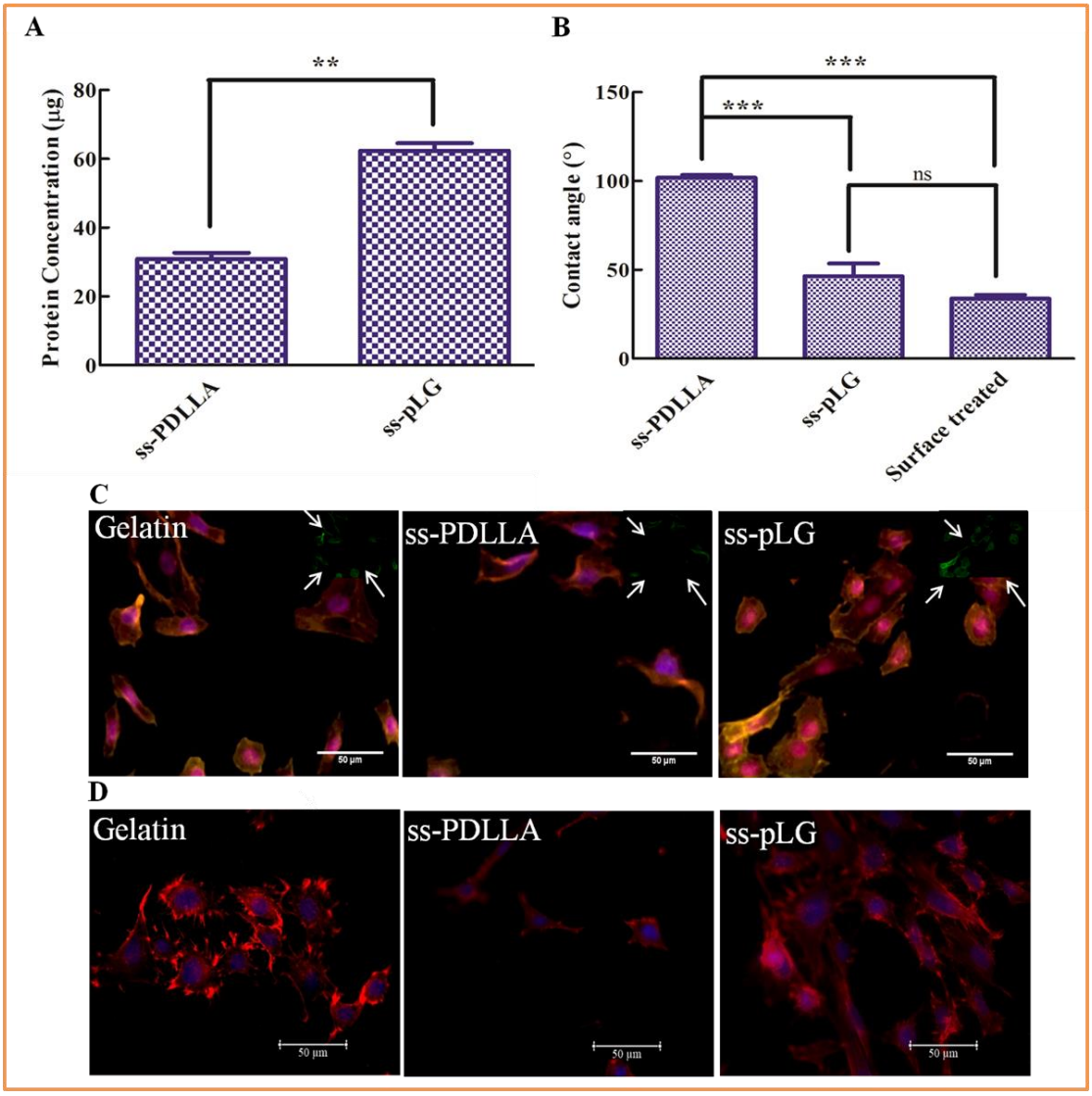

Figure 3.6. Demonstration of cell adhesion behaviour on polymer coated 2D cover glass; (A) BSA protein adsorption on to the 2D polymer film after 4 h of incubation. Protein estimation was done by using micro BCA kit. Experiments were done in triplicate and results are expressed as mean ±SD (n=3). *p <0.05, **p<0.001 ***p<0.0001 (B) Contact angle measurements of polymer coated 2D cover glass. (C) Fluorescent colocalized images of vinculin integrated with F-actin shows the adhesion of 3T3-L1 cells over the polymer coated 2D cover glass compared to that of unmodified gelatin, after 24 h of culturing. Blue shows the cell nuclei; Red shows the actin filament; Green (Inner Square) shows vinculin expression. (D) Cell spreading behaviour on 2D polymer coated cover glass.

protein associated with cell-cell and cell-matrix junctions. It is involved in the anchoring of filamentous actin (F-actin) to the membrane adhesion molecules. To evaluate the cell adhesions associated with normal physiological proteins, we chose vinculin as a model protein that was costained with actin filament and cell nuclei. . Post 24 h seeding, 3T3-L1 cells cultured on polymer coated cover glass were observed to be speroidal in shape and did not exhibit a proper shape of well-spread healthy cells. Also, actin staining revealed the intense, mesh-like red stains extended from the cell perimeter; indicating the compromised status of the cells (**Figure 3.6**C). The intensified vinculin expression at the edge of a cell indicated the presence of strong integrated adhesive sites in case of gelatin (control) and gelatin coupled PDLLA (ss-pLG) coated cover glass. Gelatin modified ss-pLG were found more effective than the unmodified polymer in terms of establishing focal contacts, since the vinculin expression was clearly seen in almost all the cells and also the cell shape were comparable with the gelatin coated cover glass. In contrast, very weak fluorescence was observed on unmodified ss-PDLLA (**Figure 3.6**C).

Thereafter, we studied the cell spreading behaviour over different polymer coated cover glass to examine the efficiency of gelatin grafting onto different arms of polymer. The morphology of adherent cells cultured on the cover glass for 48 h is shown in **Figure 3.6**D. Cells cultured on polymer coated cover glass exhibited well spread shapes and highly organized actin stress fibers. However, the extend cell adhesion was poor in case of ss-PDLLA as demonstrated by the presence of relatively lesser cell number. At the same time, cells were of more spread and polygonally elongated shape on ss-pLG, most

likely due to the strong interaction between cell-cell, which is an important property for the tissue formation.

3.2.3. Characterization of 3D scaffolds

It is proven that scaffold morphology, particularly, pore size of scaffolds influences cell invasions. However, scaffolds need interconnected pores for supporting cell invasion. Interconnectivity is also important for the nutrient supply and the formation of vascularized tissue deep within the scaffold.[108, 109] Hence it is essential to characterize the morphology and porosity of the scaffolds.

SEM images (**Figure 3.7**) show the representative porous network structures of scaffolds fabricated from gelatin modified and unmodified polymers. Lyophilized 3D scaffold of ss-pLG was distinctively different from their unmodified ss-PDLLA owing to gelatin coupling into PDLLA backbone. However, both the scaffolds exhibited heterogeneous 3D porous structure with interconnected pores. The pore size was estimated from SEM microphotographs by manual measurement of pore zones with arbitrary shapes. The mean pore diameter of ss-PDLLA and ss-pLG were found as 32.32±8.75 and 52.06±12.85 μm, respectively. On the other hand, the percentage of porosity of ss-PDLLA and ss-pLG were found as 68.3±3.4 and 66.9±12.5%, respectively Our observation reveals that the gelatin coupling to the polymer leads to increase in pore size of the 3D scaffolds. PDLLA is widely known for fabricating solid walled porous scaffolds using phase separation followed by solvent casting evaporation technique.[66] Gelatin scaffolds were also shown to have large pores after the freeze drying process.[110] In case of ss-pLG, compounded phase separation occurs between the PDLLA and gelatin. Due to this compounded phase separation, ss-pLG exhibited

higher porosity with open pore structures compared to those of unmodified ss-PDLLA. These results indicate that the mobility of hydrophilic gelatin to the side chains of PDLLA that directly affect the surface morphology of scaffolds. Overall, the outcome suggests that the covalent coupling of gelatin into PDLLA played a vital role for the increased pore size of the 3D scaffolds (**Figure 3.7**).

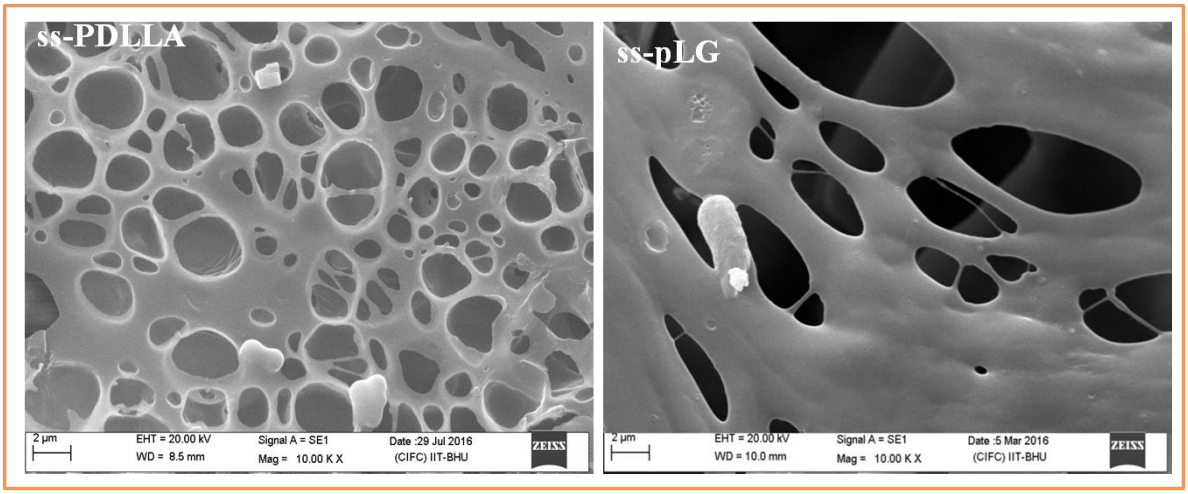

Figure 3.7 SEM Morphology of 3D scaffolds fabricated from 12% of polymer in DMSO, through freeze drying.

3.2.4. Degradation kinetics

The stability of 3D scaffolds in biological environment (which is rich in proteins and enzymes at physiological pH) will determine and validate the potential of the scaffolds for tissue engineering applications. To elucidate the role of biological environment in influencing the scaffolds configuration, lysozyme was used as a model enzyme to mimic the biological scenarios and degradation kinetics was further studied lasting for 7 days. Lysozyme is known to hydrolyze the amide group of gelatin [70] and ester groups of PLA[111]. Weight loss of both the scaffolds after day 1, 3, 5 and 7 were noted down and a plot revealing percentage of weight loss was drawn. As shown in the **Figure 3.8**A, an insignificant weight loss difference was observed in case of ss-PDLLA after 7

days of incubation in PBS whereas, ss-pLG showed noticeable but insignificant degradation after 5th day. This result reveals that the gelatin grafted and unmodified

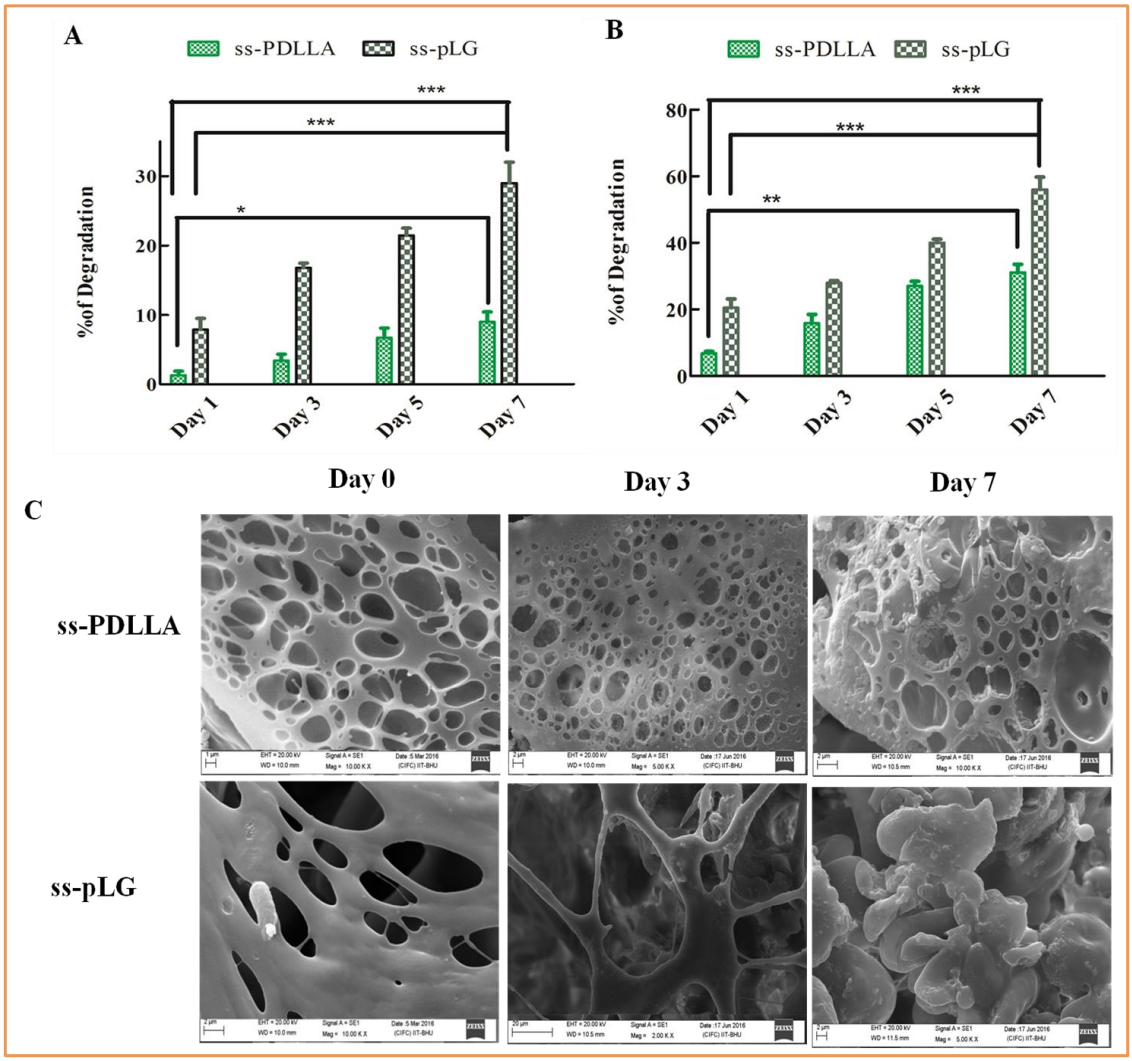

Figure 3.8. Degradation kinetics of 3D scaffolds. Comparative percentage loss of gelatin grafted and unmodified scaffolds incubated in lysozyme (A) and PBS (B) at various time interval. (C) SEM micrographs of scaffolds incubated with lysozyme *in vitro* degradation experiments in Lysozyme. Day 3 and Day 7 images of ss-pLG clearly indicate the degradation behavior of the scaffolds, whereas even in ss-PDLLA a significant change is observed.

scaffold have low susceptibility of degradation in PBS after 7 Days. However, when comparing the weight loss of scaffolds in PBS containing lysozyme, significant changes

($p<0.001$) were observed (**Figure 3.8**B). After 7 days of incubation in lysozyme, the weight loss was marginally high. For example ss-pLG showed the weight loss of 56.06±2.14 %. This observation suggests that lysozyme significantly affects the degradation of gelatin grafted ss-pLG scaffold, most likely due to enzymatic hydrolysis of the amide and ester bonds of gelatin and PDLLA. Moreover, this significantly higher degradation of scaffolds in lysozyme compared to PBS suggest, that the degradation of the scaffolds occurs mainly because of the enzymatic cleavage and also the higher degradation of ss-pLG scaffolds most likely due to the grafting of gelatin in 4 arms of ss-PDLLA backbone.

In parallel, SEM images (**Figure 3.8**C) were analysed to support our observation for the degradation behaviour of ss-PDLLA and ss-pLG polymeric scaffolds in lysozyme containing PBS medium. As clearly seen in the figure, though the porosity of the ss-PDLLA scaffold was enlarged, interconnectivity of the pores was maintained even after Day 7, whereas in case of gelatin grafted ss-pLG, the pores of the scaffolds significantly became enlarged and slowly started to lose the interconnectivity from day 3. After Day 7, interconnectivity between the pores was completely vanished and cracks started to appear on the scaffolds. The outcome thus suggests that scaffolds with larger pore sizes degrade faster as observed in case of ss-pLG. Our results are in agreement with the other authors. [67, 112] These combined quantitative and qualitative results indicate that the ss-pLG scaffold was more susceptible for enzymatic degradation followed by diffusion of hydrolyzed products into the 3D scaffolds[70, 72]. ss-pLG scaffolds affected more because of the gelatin presence in all the 4 arms of PDLLA. Higher porosity of ss-pLG could also be a reason for this degradation behaviour of the

scaffolds. Figure 3.9shows the effects of degradation based on porosity of the scaffolds.

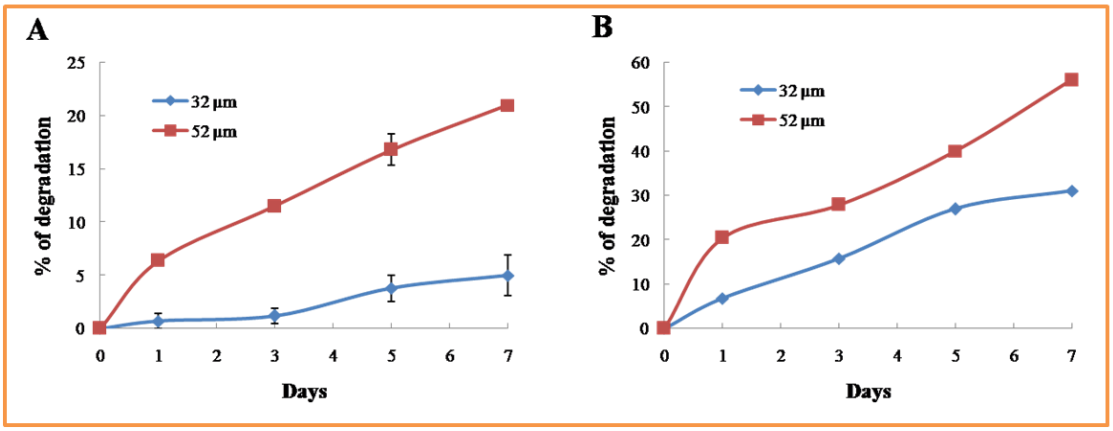

Figure 3.9. Degradation kinetics based on porosity of the scaffolds 3D scaffolds incubated in (A) PBS and (B) lysozyme containing PBS. 32 µm and 52 µm corresponds to the porosity of ss-PDLLA and ss-pLG scaffolds respectively.

Our results comply with the previous authors publications indicating that porosity influences the degradation behaviour of the scaffolds[70, 113]. Therefore, the study suggests that porosity and the hydrophilicity of the scaffolds together have influenced the 3D scaffolds to undergo degradation in the lysozyme containing PBS medium.

3.2.5. Influence of gelatin grafting on Biocompatibility and Cell-Matrix interaction of 3D scaffolds

In order to assess the survival rate of the cells grown on different forms of scaffolds (Cytocompatibility) compared to the control 2D polystyrene plate (monolayer culture), we observed the viability of 3T3-L1 cells by MTT assay. 3T3-L1 cells grown on 2D culture plate showed a significant increase in cell number on 3rd day, while a noticeable decrease in viability of the cells was observed during the further extended time points; indicating that space became the constraint limiting factor for the further growth of cells. Although, the cell growth within the 3D scaffold of ss-pLG was found

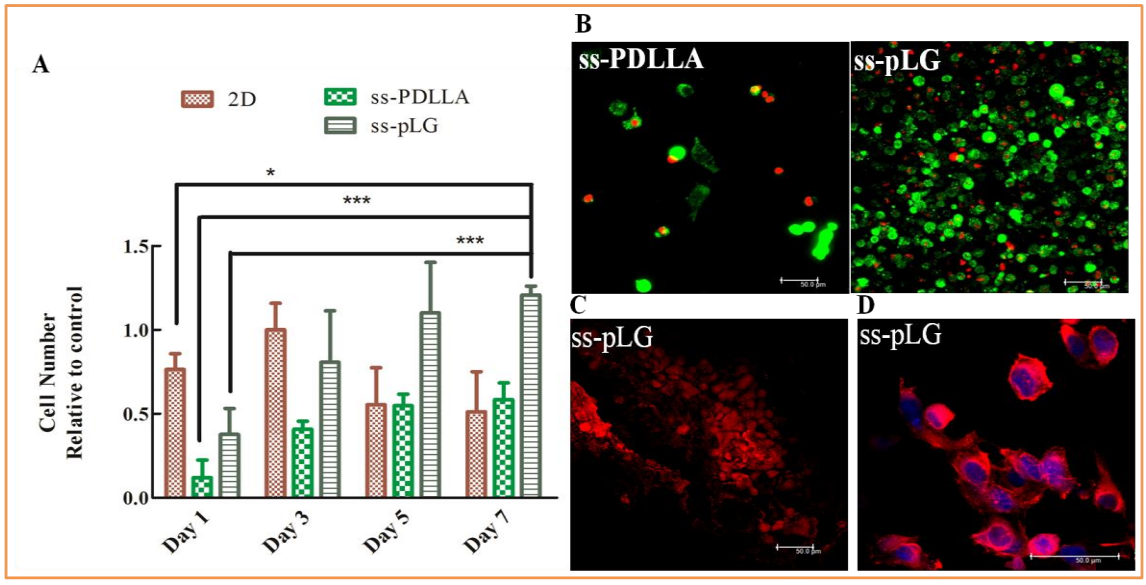

Figure 3.10. Demonstration of Biocomptability and Cell-Material interaction by the influence of gelatine coupling: (A) Cell Proliferation of 3T3-L1 within the scaffolds assessed by MTT assay, cell number was related to 1 according to the growth of cells on 2D culture plates at day 3. All bars expressed as mean values ± SD (n=3); * $p < 0.05$, **$p<0.001$ *** $p<0.0001$. (B) Representative images show viability of 3T3-L1 cells within the scaffolds after 7 days. (C) Cells cultured within the 3D scaffolds were tracked using cell tracker (Red) after 48 h. (D) Cell interconnected structures within the scaffolds. Cells were co-stained with the dyes including rhodamine phalloidin (Red) and DAPI (blue) for the observation of actin filaments and cell nuclei, respectively. Scale bar is of 50 µm.

significantly lesser compared to that of 2D monolayer culture on the 1st day, there was an increasing trend was observed till 7th day. However, the cell growth on 7th day was insignificant ($p>0.05$) compared to that of 5th day. This observation indicates that the cells utilized the whole surface of 3D porous scaffolds and therefore it remained with no free space for facilitating further growth into the scaffolds. In ss-pLG scaffold, 3.8 fold higher cell number was observed respectively, on day 7 compared to day 1. Moreover, ss-pLG scaffolds showed significantly higher degree of cell growth in comparison to the

unmodified ss-PDLLA scaffold (**Figure 3.10**A). The cell growth behaviour on scaffolds can be explained by the integrin binding sites. Such differences in the behaviour of cellular growth within the porous network of scaffolds are mainly attributed to disparity in the availability of the integrin binding sites amongst polymers. Unmodified ss-PDLLA scaffold doesn't have the integrin binding sites for the growth of cells, whereas ss-pLG scaffolds are rich in gelatin content and therefore displayed higher cell growth**.** Furthermore, the spacing between integrin binding sites of adhesive ligand (i.e ss-pLG) might be 70 nm or lesser than 70 nm, since it has been demonstrated that when the average ligand spacing is larger than 70 nm cell adhesion is "turned off" and for instance when the ligand spacing is of 70 nm cell adhesion mechanism gets "turned on" and subsequent cellular processes occur [114-116].

Cell viability was also assessed through Confocal Laser Scanning Microscope (CLSM) using live/ dead cell staining kit. **Figure 3.10**B shows the viability of cells cultured within the scaffolds after 7 days of seeding. This study revealed that the cell number present within the ss-pLG scaffolds were notably higher compared to that of unmodified ss-PDLLA. This qualitative result is in good agreement with the MTT data revealing that, ss-pLG significantly supports the cell adhesion as well as their proliferation. Very few dead cells were seen in case of gelatin modified scaffold, mainly due to the insufficient space within the scaffolds whereas incase of unmodified polymeric scaffold, the adhered cells lost the contact because of the absence of integrin binding sites. MTT assay in combination with live/dead staining assays led us to conclude that gelatin coupling on to PDLLA promoted the cellular viability significantly that directly implies the improved proliferation of 3T3-L1 cells on ss-pLG scaffolds.

It is known that scaffolds having pore size lesser than 25 μm will affect the cell migration and cell distribution on the scaffolds, thereby affecting the cell-cell interaction[117]. ss-pLG scaffold exhibited pore sizes significantly larger than the size of 3T3-L1 cells (**Figure 3.10**C), indicate that cells were not exposed for steric hindrance and prone to migrate throughout the 3D matrix, a phenomenon known as contact guidance.[118]

In order to evaluate the biocompatibility of the modified ss-pLG scaffolds, morphologies of 3T3-L1 cells were observed after 48 h of culture through staining of actin filaments. Image exhibits clear interconnectivity of the cells grown within the 3D scaffolds (**Figure 3.10**D). ss-pLG scaffold showed elongated morphology with good adherence and spreading. Moreover, clustering of cells as demonstrated by the arrangement of their actin fibers was observed in ss-pLG scaffold suggesting that gelatin onto the ss-PDLLA arms induces the aggregation of cells.

3.2.6. Influence of gelatin grafting on Hemocompatability

3.2.6.1. Hemolysis

Hemolysis is one of the important problems associated with the compatibility of biomaterials since RBCs will be lysed even when they come in contact with water. Therefore, developed biomaterials should preserve the integrity and functionality of erythrocytes in whole blood samples. Hemolysis of the tested scaffolds for 1 h and 8 h compared with the control PBS solution is shown in **Figure 3.11**A. All of our fabricated scaffolds were found hemocompatible since the percentage of hemolysis is lesser than 3 %. It was reported that up to 10% hemolysis is permissible for biomaterials [119].

Moreover, the gelatin grafted ss-pLG showed higher percentage of hemolysis, but differences in their levels of hemolysis were quite insignificant ($p>0.05$) compared to that of ss-PDLLA polymeric scaffold and negative control (i.e., PBS). Furthermore. there was no significant difference ($p>0.05$) in the levels of hemolysis observed during the extended period in case of modified and unmodified scaffolds with respect to PBS.

3.2.6.2. Evaluation of erythrocyte membrane integrity

Membrane integrity of erythrocytes when incubated with the 3D scaffolds was evaluated by quantifying the enzyme LDH (**Figure 3.11**B). In this experiment leukocytes and plasma were removed from whole blood where, only RBCs suspended in PBS were used to quantify the LDH released from the cells. At the end, possible disturbances in membrane integrity of erythrocytes by the scaffolds were observed. Scaffolds incubated erythrocytes did not show any significant increase ($p>0.05$) in LDH release when compared to PBS (negative control) after 1 h and 8 h interval. In **Figure 3.11**B significance different level at 8 h between all the scaffolds compared with PBS is shown. This result indicated that the scaffolds maintain the membrane integrity of erythrocytes and did not cause any damage to the cell membrane.

3.2.6.3. Activated Partial Throboplastin Time (APTT) and Prothrombin Time (PT)

The blood coagulation cascade includes intrinsic, extrinsic and common pathways. APTT and PT are mainly used to examine the intrinsic and extrinsic pathways, respectively. The APTT test has been widely used for clinical detection of the abnormality of blood plasma and for the primary screening of anticoagulative

chemicals. **Figure 3.11**C demonstrates the effects of gelatin grafted and unmodified scaffolds on APTT in blood plasma. Significant difference in coagulation time was

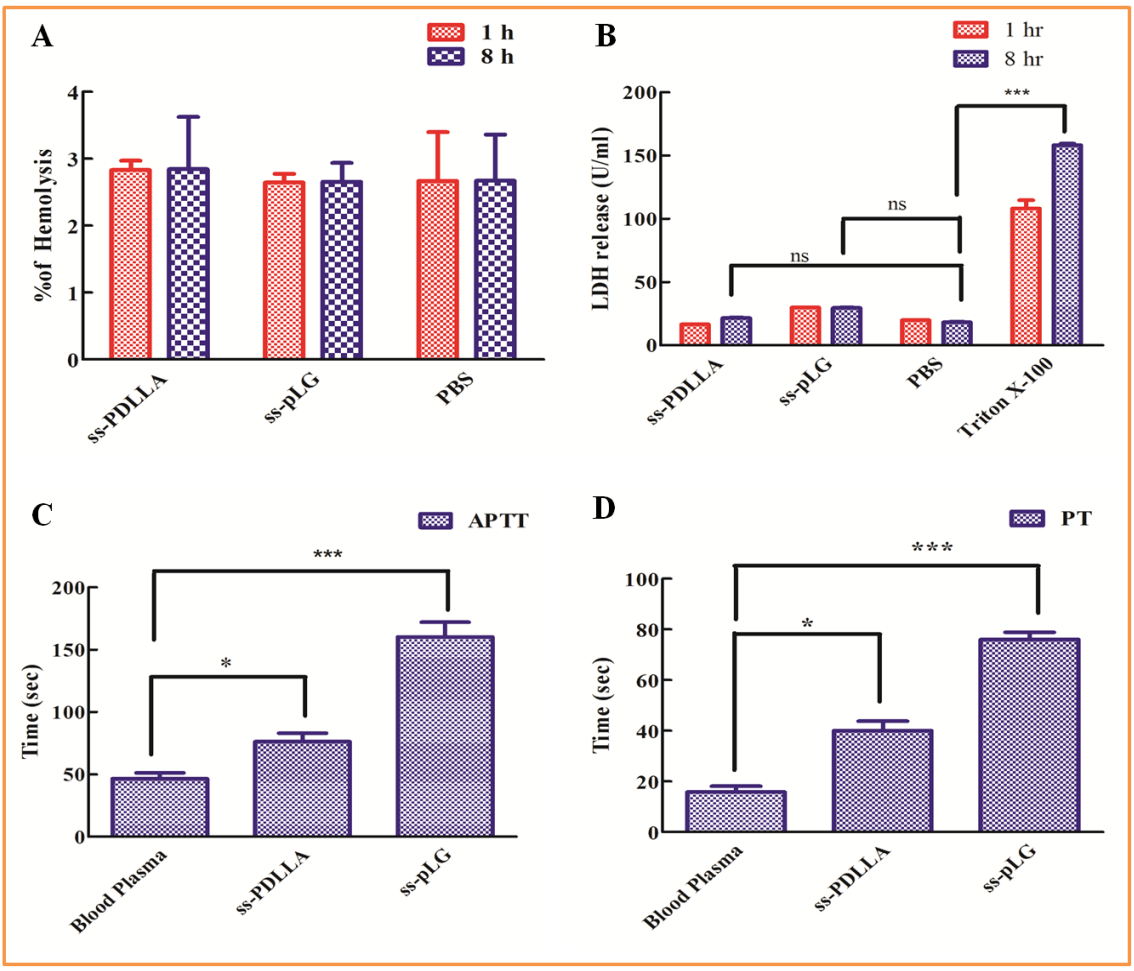

Figure 3.11. Hemocompatability of ss-pLG based 3D scaffolds (A) Hemolysis of the scaffolds after 1 h and 8 h, no significant difference were observed in comparison to that of PBS; (B) Erythrocytes membrane integrity in presence of scaffolds by LDH release assay, compared to 1% Triton X-100 and PBS as positive and negative control. Effects of gelatin grafted and unmodifed scaffold on Activated Partial Thromboplastin Time (C) and Prothrombin Time (D) were compared with control blood plasma. All bars are expressing mean values± SD (n=3); ns- nonsignificant;* $p<0.05$; *** $p<0.0001$.

found between the control blood plasma and the unmodified ss-PDLLA scaffolds ($p < 0.05$). Notably, ss-pLG scaffolds incubated in blood plasma showed delayed coagulation, as compared to control blood plasma ($p<0.0001$).

The effects on the extrinsic pathway of blood coagulation can be better evaluated by measuring the time till fibrin clot forms. Trend of PT was found similar to that of APTT (**Figure 3.11**D), when the scaffolds were incubated in blood plasma. In contrast, the clotting time was found nearly half. Our results are in good agreement with other research group results [73], indicating that delayed activation of intrinsic and extrinsic blood coagulation pathway was due to the hydrophilic nature of the scaffolds (ss-pLG).[120, 121]

3.3. CONCLUSION

Here, we have synthesized an efficient biocompatible and hydrophilic polymer with cell adhesive surface using combined ROP followed by end functionalization using carbodimide chemistry, which was confirmed by ^{1}H NMR and FTIR. Improved thermal behaviour of ss-pLG compared to its unmodified polymer ss-PDLLA was also characterized by TGA and DSC. End functionalization of gelatin onto the PDLLA backbone improved the cell adhesion property and the tuning of the cell adhesion was achieved by gelatin coupling on to 4 arms of PDLLA polymer (ss-pLG). 3D scaffolds prepared from unmodified ss-PDLLA and gelatin grafted ss-pLG polymers showed remarkably good compatibility to 3T3-L1 cells and blood RBCs. ss-pLG scaffolds facilitated improved cell proliferation with interconnected cellular morphology within the 3D matrix. Degradation kinetics revealed that half of the ss-pLG scaffold was degraded after 7 days in lysozyme medium owing to their hydrophilicity nature. This

hydrophilicity also affected the blood coagulation time as demonstrated by the measurement of APTT and PT. Thus, this modular approach of developing polymers with cell adhesive surface can be efficiently utilized to create 3D scaffolds for the successful applications where cell depots are used. In addition, the burst release of biomolecule from the scaffold matrix can be utilized for growth factor delivery and wound healing applications.